

## ACCELERATION AMPLIFIED AND DE-AMPLIFIED RESPONSES WITHIN GEOSYNTHETIC-REINFORCED SOIL STRUCTURES

E. Y. Kencana<sup>1</sup>, K. H. Yang<sup>2</sup>, and W. Y. Hung<sup>3</sup>

<sup>1</sup>Graduate Research Assistant (Corresponding Author); Department of Construction Engineering, National Taiwan University of Science and Technology, No. 43 Keelung Road, Section 4, Taipei 106, Taiwan, R.O.C.;  
Tel: +886-9 216 04945; Email: Erick\_ykLie@yahoo.com,

<sup>2</sup>Assistant Professor, Department of Construction Engineering, National Taiwan University of Science and Technology, No. 43 Keelung Road, Section 4, Taipei 106, Taiwan, R.O.C.; Tel: +886-2 273 01227;  
Fax: +886-2 273 76606; Email: khy@mail.ntust.edu.tw,

<sup>3</sup>Associate Technologist, National Center for Research on Earthquake Engineering, No. 200, Sec. 3, Xinhai Rd., Taipei 106, Taiwan, R.O.C.; Tel: +886-9 553 29820; Fax: +886-3 425 2960; Email: wyhung@ncree.narl.org.tw.

### ABSTRACT

Physical data from various dynamic centrifuge modeling and shaking table tests on geosynthetic-reinforced soil (GRS) structures are compiled and used to evaluate the acceleration amplified and de-amplified responses within GRS structures. Analysis results show the horizontal acceleration ( $a_h$ ) inside GRS structures has a non-uniform distribution with height and varies with maximum input acceleration ( $a_{max}$ ). The variation and magnitude of acceleration amplification factor ( $A_m$ ), the ratio of  $a_h$  to  $a_{max}$ , decrease with the increasing  $a_{max}$ . The horizontal acceleration inside GRS structures amplifies mostly at approximately  $a_{max} < 0.40g$  and attenuates at  $a_{max} > 0.40g$ . The results also show the acceleration amplified and de-amplified responses are highly dependent on acceleration frequency  $f$ . The acceleration inside GRS structures amplifies considerably when the predominant and fundamental frequencies are close. Further, this paper examines the  $A_m$  and  $a_{max}$  relationships (i.e.,  $A_m = 1.45 - a_{max}/g$ ), proposed based on a series of finite element simulations and adopted in the current GRS structure design guidelines. The comparative results indicate  $A_m$  and  $a_{max}$  relationships adopted in the current design guidelines follow the lower bound of the physical data compiled in this paper, specifically for underestimate of  $A_m$  at lower  $a_{max}$ . The results obtained from this study provide insightful information for seismic design of GRS structures.

*Keywords: Acceleration amplification; geosynthetic-reinforced soil; dynamic centrifuge test; shaking table.*

### INTRODUCTION

Geosynthetic-reinforced soil (GRS) retaining structures have been proved to exhibit good performance against seismic loadings (e.g., Tatsuoka et al. 1995). Conventionally, seismic stability analyses of GRS structures are developed within the framework of a pseudo-static approach. In this approach, horizontal acceleration ( $a_h$ ) within GRS structures is one of the important parameters to evaluate seismic earth pressure by Mononobe-Okabe method. As seismic waves pass through ground to GRS structures, the amplification or attenuation of the horizontal acceleration  $a_h$  relatively to the maximum input acceleration ( $a_{max}$ ) has been reported by several researches using the methods of numerical simulations (Bathurst and Hatami 1998), shaking table tests (Huang et al. 2010, Krishna and Latha 2007, Matsuo et al. 1998) and dynamic centrifuge modeling tests (Hung et al. 2011, Liu et al. 2010).

Current GRS structure design guidelines (i.e., Elias et al.(2001), NCMA (2010)) conventionally

assume  $a_h$  is uniformly distributed with structural height and can be calculated from acceleration amplification factor  $A_m$ , the ratio of  $a_h$  to  $a_{max}$ , as shown in Eq. 1:

$$A_m = (1.45 - a_{max} / g) \quad (1)$$

where  $A_m$ ,  $a_{max}$  and  $g$  are acceleration amplification factor, maximum input acceleration and gravity, respectively. The  $A_m$  and  $a_{max}$  relationships adopted in the current design guidelines were proposed by Segrestin and Bastick (1988) based on a series of finite element simulations of steel reinforced soil walls up to 10.5m high that were subjected to ground motions with a very high predominant frequency of 8Hz. However, to the best of the authors' knowledge, the assumed  $a_h$  distribution with height and the proposed  $A_m$  and  $a_{max}$  relationships have not been extensively examined by physical data yet.

In this study, a series of dynamic centrifuge modeling on GRS structures were performed to

investigate the dynamic behavior of GRS structures. Besides, an experimental database from various dynamic centrifuge and shaking table tests in the literature are developed. One of the objectives of this study is to use the compiled physical data in the database to evaluate the acceleration amplified and de-amplified responses within GRS structures. The other objective is to examine the suitability and applicability of the currently available seismic design methods in the GRS structure design guidelines. The results obtained from this study are expected to provide insightful information and design implications for the seismic design of GRS structures.

## DATABASE OF GRS STRUCTURE DYNAMIC RESPONSES

### Dynamic Centrifuge Modeling Test

A series of dynamic centrifuge modeling tests were conducted at National Central University (NCU) in Taiwan to study the dynamic behavior of GRS embankments (Hung et al. 2011). All the embankment models were 160 mm tall, 367mm wide at top and with the facing slope 1 vertical to 1 and 0.5 horizontal, respectively. This embankment configuration represents a 8 m high and 18.35m wide in prototype at target gravity level of 50g. Figure 1 shows the configuration of the embankment model. Dry fine pure quartz sand was used as backfill material. The fine pure quartz sand was classified as poor sand (SP) according to unified soil classification system (USCS) with  $D_{50} = 0.19$  mm,  $\gamma_{d,max} = 16.3$  kN/m<sup>3</sup>,  $\gamma_{d,min} = 14.1$  kN/m<sup>3</sup>, and  $G_s = 2.65$ . The backfill unit weight was  $\gamma = 15.1$  kN/m<sup>3</sup> and soil friction angle  $\phi = 38^\circ$  at the target relative density  $D_r = 53\%$ .

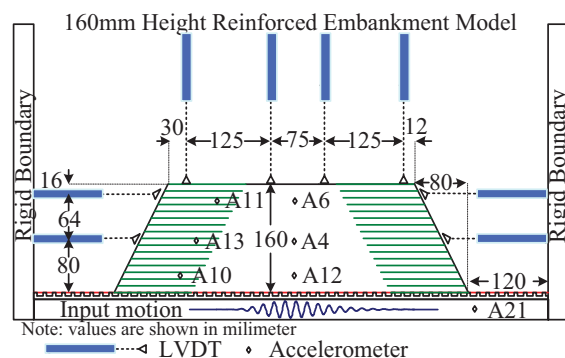


Fig. 1 Configuration and instrument layouts of centrifuge GRS model.

The reinforcement used in the centrifuge model was a noncommercial nonwoven geotextile which has ultimate tensile strength  $T_{ult} = 2.24$  kN/m (corresponding to  $T_{ult} = 112$  kN/m in prototype scale)

obtained from the wide-width strip tensile test (ASTM D4595). Ten layers of reinforcement were evenly distributed inside the centrifuge model and folded backward to form a wrapped-around facing.

The embankment model was instrumented with accelerometers and linear variable differential transformers (LVDTs) to monitor the acceleration inside the reinforced and retained areas and to measure the structural deformation, respectively. While the layer by layer construction continued, the accelerometers, indicated as “A” in Figure 1, were placed at top, middle and lower areas of the embankment models. After the model construction was completed, the LVDTs were positioned on the model. The centrifuge models were subject to sinusoidal base motions with two different frequencies  $f = 1$  Hz and 4.8 Hz and the magnitude of base motion  $a_{max}$  ranging from 0.02g to 0.27g. A total of 15 sinusoidal cycles were applied to each  $a_{max}$ . The blue line in Fig. 2 shows one of input base acceleration with 4.8Hz and the black line is the acceleration history measured at top of reinforced area in GRS embankment model. The fundamental frequency of embankment model was monitored to be about  $f = 5.6$  Hz.

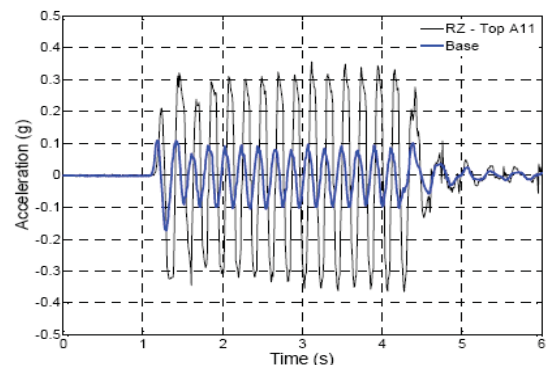


Fig. 2 Input acceleration (blue line) with  $f = 4.8$ Hz and  $a_{max} = 0.1$ g and acceleration measured at top of reinforced area in GRS embankment model (black line)

### Other Seismic Test Data

Other seismic test data collected from various dynamic centrifuge modeling tests and shaking table tests (Huang et al. 2010, Krishna and Latha 2007, Matsuo et al. 1998, Nova-Roessig and Sitar 2006) were compiled into database. A total of 5 GRS structure cases were presented. Key properties and parameters for each of the dynamic GRS structure tests referenced in this paper are summarized in Table 1, including the structure type, geometry, backfill and reinforcement material and seismic characteristics (e.g., maximum input acceleration  $a_{max}$  and frequency  $f$ ). Readers are noted that all numbers shown in Table 1 are presented in the prototype scale.

Table 1 Summary of dynamic GRS structure tests

Category	Factor	Symbol (unit)	This study	Nova-Roessig and Sitar (2006)	Database Matsuo et al. (1998)	Krishna and Latha (2007)	Huang et al. (2010)
General	Test		Dynamic centrifuge	Dynamic centrifuge	Shaking table	Shaking table	Shaking table
	Structure type		Embankment	Embankment	Wall and Slope	Wall	Slope
Geometry	Height	$H$ (m)	8	7.3	0.98, 1, 1.4	0.6	0.48
	Facing inclination	$\beta$ (degree)	63.4 and 45	90 and 63.4	90 and 78.6	90	60
	Facing type		Wrap-around facing	Wrap-around facing	Wooden panel	Wrap-around facing	Aluminum plate
Backfill	Backfill		Fine quartz sand	Monterey #30 sand	Toyoura sand	Local India sand	Rhombically steel rod
	Unit weight	$\gamma$ (kN/m <sup>3</sup> )	15	15.6 and 16.2	13.55, 15 and 16.49	18	68.5
	Initial relative density	$D_r$ (%)	53	55 and 75	60	34-37	N/A
Reinforcement	Reinforcement		Nonwoven geotextile	Geotextile and wire mesh strip	Geogrid	Nonwoven geotextile	Nonwoven geotextile
	Length to wall height ratio	$L/H$	0.7	0.7 and 0.9	0.4 and 0.7	0.7	0.83
	Number of reinforcements	$n$	10 and 16	10	5 and 7	2, 3 and 4	3
	Stiffness at 2% strain	$J_{2\%}$ (kN/m)	112 <sup>a</sup>	8.3, 19.3 and 138	480, 901 <sup>a</sup>	152	50
Seismic characteristics	Input motion type		Sinusoidal	Sinusoidal and Earthquake wave	Sinusoidal and Earthquake wave	Sinusoidal	Single-cycle sinusoidal
	Max. input motion	$a_{max}$ (g)	0.02-0.27	0.11 - 1.08	0.05 - 0.625	0.1 - 0.2	0.1 - 1
	Frequency	$f$ (Hz)	1 and 4.8	1.5 - 7.5	1-2 and 5	1-3	3, 6 and 15

<sup>a</sup>the reinforcement stiffness is calculated at failure strain

## RESULTS AND DISCUSSIONS

In this section, the physical data compiled from 5 GRS structure cases are used to evaluate the influence of factors on acceleration amplified and de-amplified responses within GRS structures, specifically for the acceleration amplification factor  $A_m$ . Among all of the factors in Table 1, the maximum input acceleration  $a_{max}$ , location  $z$  and seismic frequency  $f$ , are identified to have the most significant influence on  $A_m$ . Details of the influence of these factors on  $A_m$  are discussed as follows.

### Influence of maximum input acceleration on $A_m$

Figure 3 presents the influence of  $a_{max}$  on  $A_m$  at top area of GRS structures. Because Matsuo et al. (1998) only measured the acceleration at the midheight of the reinforced soil mass, their data is not included in Figure 3. From this figure, it can be seen that the variation and magnitude of  $A_m$  decrease with the increasing  $a_{max}$ . Large variation at relatively low  $a_{max}$  (i.e., < 0.2g) is likely because the influence from other factors, particularly for seismic frequency  $f$ , becomes more profound at low  $a_{max}$ . The influence of seismic frequency  $f$  on  $A_m$  is discussed later. A power trend line (i.e.,  $A_m = 0.605 a_{max}^{-0.315}$ ) is plotted in

Figure 3 to depict the overall relationships between  $a_{max}$  and  $A_m$ . In general, the crossover point between amplification and attenuation occurs at  $a_{max}$  value of about 0.40g. Strong base motion ( $a_{max} \geq 0.40g$ ) results in acceleration de-amplification inside GRS structures.

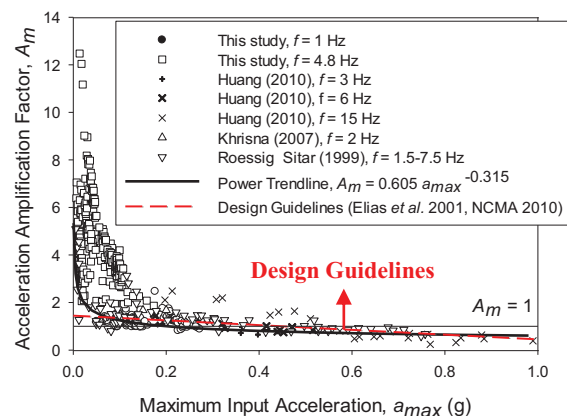


Fig. 3 Relationship of acceleration amplification factor and maximum input acceleration at top area of GRS structures.

The acceleration amplified and de-amplified responses with  $a_{max}$  are likely associated to the increase of plastic/permanent displacement of structures with increasing  $a_{max}$ . Matsuo et al. (1998) pointed out that an amplified response occurs under a small displacement state and a de-amplified response under a large displacement state. This implies the amplification characteristics of GRS structures are influenced by the integrity status of the structures. Huang et al. (2010, 2011) found transitions from an amplification state to a de-amplification state at a relatively intensive input base acceleration of 0.4g-0.6g, which are associated to the development of major slip planes in the slope (or to the noticeable slope displacement).

The data are further used to examine the  $A_m$  and  $a_{max}$  relationships (i.e.,  $A_m=1.45-a_{max}/g$ ) adopted in current two GRS structure design guidelines (Elias et al. 2001 and NCMA 2010). The  $A_m$  and  $a_{max}$  relationships in Equation 1 results in the horizontal acceleration inside GRS structures amplification (i.e.,  $A_m>1$ ) at  $a_{max}<0.45g$ . This result is very close to the result determined from the physical data in Figure 3. What is more important, the  $A_m$  and  $a_{max}$  relationships in the design guidelines seem to follow the lower bound of the  $A_m$  data in Figure 3. This would lead to an underestimation of  $A_m$  especially at lower  $a_{max}$  and, consequently, overestimation of the seismic stability of GRS structures. The influence of system stiffness may be used to explain why the  $A_m$  and  $a_{max}$  relationships in the design guidelines follows the lower bound of the  $A_m$  data. It is because the system stiffness of the steel reinforced structure used to establish the  $A_m$  and  $a_{max}$  relationships in the design guidelines is relatively stiffer than those of GRS structures presented in this study. The shaking table test results by El-Emam and Bathurst (2007) indicated that increasing the system stiffness of the model structure led to a decrease in the magnitude of acceleration amplification factors.

#### Influence of Location on $A_m$

Figure 4 shows variation of  $A_m$  with elevation inside GRS structures. The values of  $A_m$  are obtained by averaging all  $A_m$  data from database at the top, middle and lower areas of the GRS structures separately. It can be observed from this figure that the distribution of  $A_m$  with height inside GRS structures is non-uniform and varies with  $a_{max}$ . The acceleration amplified and de-amplified responses magnify with elevation. Acceleration amplifies ( $A_m>1$ ) and the magnitude of  $A_m$  increases with elevation at approximately  $a_{max}<0.40g$ . Acceleration de-amplifies ( $A_m\leq 1$ ) and the magnitude of  $A_m$  decreases with elevation at approximately  $a_{max}\geq 0.40g$ .

The results indicates that the design of GRS structures against seismic loading needs to consider

the change of acceleration with height. That is because an uniform distribution of  $A_m$  with height is conventionally assumed in current design guidelines (i.e., Elias et al.(2001), NCMA (2010)) to evaluate the seismic stability of GRS structures. However, the assumption is inconsistent with the observation in the present study. The assumed uniform distribution of  $A_m$  with height may be validated at  $a_{max}\geq 0.30g$  in which the non-uniform distribution of  $A_m$  with height is not obvious, as shown in Fig. 4. For  $a_{max}<0.30g$ , the assumption of uniform distribution may underestimate the  $A_m$  at top few layers of GRS structures and results in overestimating the local stability around these areas. Specifically, the effect of amplification coupled with low confinement can cause local breakage and pullout failure at top few layers of reinforcement.

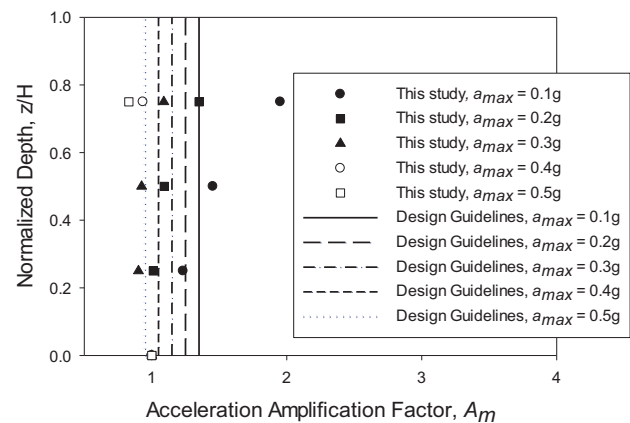


Fig. 4 Variation of  $A_m$  with elevation within GRS structures.

#### Influence of Frequency on $A_m$

The acceleration amplified and de-amplified responses significantly vary with acceleration frequency. This observation is demonstrated in Figs. 5a and 5b by the data from this study and Huang et al. (2010), respectively. These figures clearly show the  $A_m$  increases with the increasing seismic frequency  $f$  or frequency ratio  $F_r$ , defined as the predominant frequency of seismic wave divided by the fundamental frequency of structures. It can be seen that the acceleration inside GRS structures amplifies considerably when the predominant frequency is close to the fundamental frequency (i.e.,  $F_r$  close to 1.0). Clearly, acceleration response inside GRS structures is highly dependent on the seismic frequency. However, the effect of frequency on  $A_m$  has not been considered in the current design methods like Equation 1. Methods for including the effect of frequency on  $A_m$  into Equation 1 deserve further investigation.

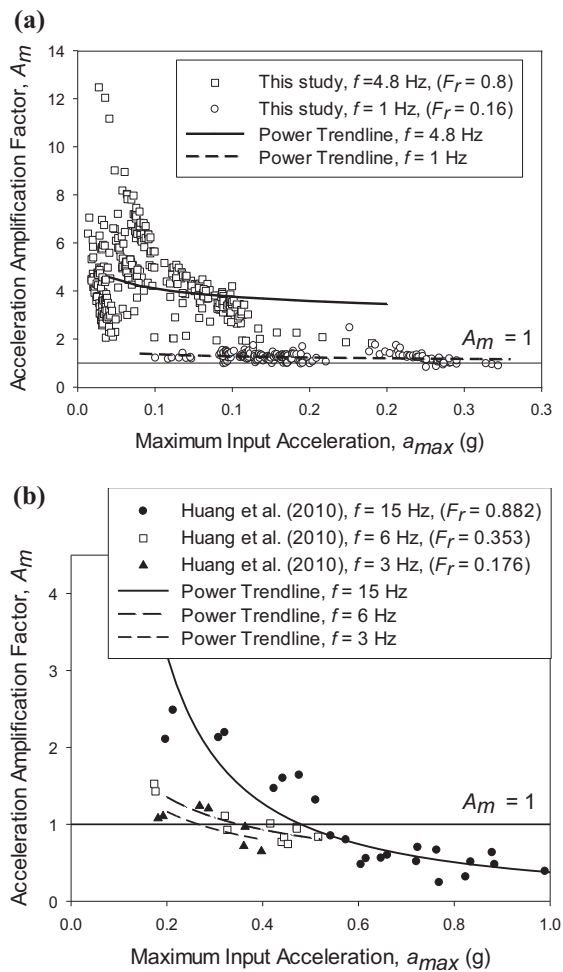


Fig. 5 Influence of frequency on  $A_m$ : (a) this study; (b) Huang et al. (2010)

## CONCLUSIONS

In this study, physical data from various dynamic centrifuge modeling tests and shaking table tests on geosynthetic-reinforced soil (GRS) structures were compiled and used to evaluate the acceleration amplified and de-amplified responses within GRS structures, specifically for the acceleration amplification factor  $A_m$ . This study identified that the amplification characteristics of GRS structures were highly dependent on the maximum input acceleration  $a_{max}$ , elevation within GRS structures  $z$  and seismic frequency  $f$ . The specific conclusions on the influence of these three factors on  $A_m$  and the relevant design implications drawn from this study are as follows:

1. The variation and magnitude of  $A_m$  decrease with the increasing  $a_{max}$ . Large variation at relatively low  $a_{max}$  (i.e.,  $a_{max} \leq 0.20$ ) is likely because the influence from other factors, particularly for seismic frequency  $f$ , becomes more profound. Overall, the horizontal acceleration inside GRS structures

amplifies ( $A_m > 1$ ) mostly at approximately  $a_{max} < 0.40g$  and de-amplifies ( $A_m < 1$ ) at  $a_{max} \geq 0.40g$ . The  $A_m$  and  $a_{max}$  relationships in the current design guidelines seem to follow the lower bound of the  $A_m$  data compiled in this study, which would lead to an underestimate of  $A_m$  at low  $a_{max}$  and, consequently, overestimate the seismic stability of GRS structures.

2. The non-uniform distribution of  $A_m$  with height inside GRS structures was observed in this study. The acceleration amplified and de-amplified responses enhance with height. The uniform distribution of  $A_m$  with height assumed in the current design guidelines may underestimate the  $A_m$  at top few layers of GRS structures and results in overestimating the local stability around these areas.

3. This study found acceleration responses are highly dependent on the seismic frequency. The  $A_m$  increases with the increasing seismic frequency  $f$  and acceleration amplifies considerably when the predominant frequency is close to the fundamental frequency.

## REFERENCES

- ASTM D4595. Standard Test Method for Tensile Properties of Geotextiles by the Wide-Wide Strip Method. The American Society for Testing and Materials. West Conshohocken, PA.
- Bathurst, R. J. and Hatami, K. (1998). Seismic response analysis of a geosynthetic-reinforced soil retaining wall. *Geosynthetics International*, 5(1-2):127-166.
- El-Emam, M. and Bathurst, R.J. (2007). Influence of reinforcement parameters on the seismic response of reduced-scale reinforced soil retaining walls. *Geotextiles and Geomembranes*, 25(1):33 - 49.
- Elias, V., Christopher, B.R. and Berg, R.R. (2001). Mechanically Stabilized Earth Walls and Reinforced Soil Slopes Design and Construction Guidelines, Report No. FHWA-NHI-00-043, National Highway Institute, Federal Highway Administration, Washington, D.C.
- Huang, C.-C., Horng, J.-C., Chueh, S.-Y., Chiou, J.-S. and Chen, C.-H. (2011). Dynamic behavior of reinforced slopes: horizontal displacement response. *Geotextiles and Geomembranes*, 29:257-267.
- Huang, C.-C., Horng, J.-C., Chueh, S.-Y., Chiou, J.-S. and Chen, C.-H. (2010). Dynamic behavior of reinforced slopes: horizontal acceleration response. *Geosynthetics International*, 17(4):207-219.

- Hung, W.-Y., You, T.-R., Chiou, Y.-Z., Hwang, J.-H., Lee, C.-J., Chiou, J.-S. and Chen, C.-H. (2011). Centrifuge modeling on seismic behavior of reinforced earth embedment. Proc. 14th Conference on Current Researches in Geotechnical Engineering in Taiwan
- Krishna, A. M. and Latha, G.M. (2007). Seismic response of wrap-faced reinforced soil-retaining wall models using shaking table tests. *Geosynthetics International*, 14(6):355-364.
- Liu, H., Wang, X. and Song, E. (2010). Centrifuge testing of segmental geosynthetic-reinforced soil retaining walls subject to modest seismic loading. Proc. GeoFlorida 2010: Advances in Analysis, Modeling and Design: 2992-2998.
- Matsuo, O., Tsutsumi, T., Yokoyama, K. and Saito, Y. (1998). Shaking table tests and analysis of geosynthetic-reinforced soil retaining walls. *Geosynthetics International*, 5(1-2):97-126.
- NCMA (2010). Design Manual for Segmental Retaining Walls, National Concrete Masonry Association Herndon, VA.
- Nova-Roessig, L. and Sitar, N. (2006). Centrifuge model studies of the seismic response of reinforced soil slopes. *Journal of Geotechnical and Geoenvironmental Engineering*, 13(3):388-400.
- Segrestin, P. and Bastick, M., J. (1988). Seismic design of reinforced earth retaining walls - The contribution of finite elements analysis. Proc. Intl. Geotechnical Symposium on Theory and Practice of Earth Reinforcement: 577 - 582.
- Tatsuoka, F., Koseki, J. and Tateyama, M. (1995). Performance of geogrid-reinforced soil retaining walls during the Great Hanshin-Awaji earthquake, January 17, 1995. Proc. International Conference on Earthquake Geotechnical Engineering, IS Tokyo '95:55 - 62.